ISSN 3048-8222 (Online) | www.ijsate.com | editor@ijsate.com

International Journal of
Science, Architecture, Technology and Environment

Error Evaluation of Line-of-Sight Angle Tracking System for Random Maneuvering Targets Using the Extended Kalman Filter and the Unscented Kalman Filter

Ngo Trung Toan[1*]

[1]Missile Faculty, Air Defence-Air Force Academy, Ha Noi, Viet Nam

*Corresponding author email: Huyndai55@gmail.com

DOI: https://doi.org/10.63680/ijsate0526006.6

Abstract

This paper presents an error evaluation method for the Line-of-Sight (LOS) angle tracking system under conditions of randomly maneuvering targets, using two common filtering algorithms: the Extended Kalman Filter (EKF) and the Unscented Kalman Filter (UKF). The dynamic model of the system is established in a discrete nonlinear form, taking into account the effects of target maneuvering factors, measurement errors, and random noise. Based on simulation results, the paper analyzes the estimation errors of LOS angle, angular rate, and target acceleration. The obtained results serve as a basis for optimizing controllers and improving the accuracy of modern LOS tracking control systems.

Keywords: Extended Kalman Filter, Unscented Kalman Filter, Line-of-Sight tracking, Randomly maneuvering target, Nonlinear system, Error evaluation, EKF, UKF, LOS.

1. Introduction

In target tracking control systems, especially in radar, air defense, and guided missile systems, accurately determining the LOS angle is a key factor ensuring precise tracking and interception capability. However, under conditions where the target performs random maneuvering motions with complex varying accelerations and is affected by measurement noise, accurately estimating the LOS angle and angular rate becomes highly challenging. Traditional linear filters such as the Kalman Filter achieve high effectiveness only when the system model is nearly linear. When the system exhibits strong nonlinearity, the EKF and UKF are commonly applied to improve estimation quality. The EKF linearizes the model around an operating point, while the UKF uses a set of sigma points to propagate the entire probability distribution through the nonlinear function, thereby better capturing the system's nonlinear characteristics. This paper focuses on comparing and evaluating the estimation errors of the LOS angle tracking system when applying the two above filtering methods, in which the target model is constructed based on sinusoidal maneuvering motion with random factors. Through numerical simulations, the paper analyzes detailed error evaluation criteria to determine the effectiveness of each filter under different operating conditions, thereby providing guidance for selecting the appropriate filtering algorithm for practical LOS tracking systems.

2. Algorithm Synthesis

2.1. Discrete Nonlinear Model Construction

The LOS tracking system is responsible for determining and maintaining the observation direction from the missile to the target in space. Considering the relative motion between the missile and the target in the control plane, we have:

$$\dot{D}_m = V_m \cos(\varphi_n - \vartheta_m) - V\cos(\varphi_n - \vartheta) \tag{1}$$

$$D_m \omega_n = V\sin(\varphi_n - \vartheta) - V_m \sin(\varphi_n - \vartheta_m) \tag{2}$$

Where:

D_m : distance to the target (m);

V_m , V : velocities of target and missile (m/s);

φ_n : LOS angle (deg);

ω_n : LOS angular rate (deg/s);

ϑ_m , ϑ : heading angles of target and missile (deg).

Taking the derivative of (2) with respect to time and transforming, we obtain the relationship between the LOS angular rate ω_n, distance D_m and the normal accelerations of the target j_m and the missile j_T :

$$\dot{\omega}_n = \frac{1}{D_m}(V_m \dot{\vartheta}_m - V\dot{\vartheta}) - \frac{2\dot{D}_m}{D_m}\omega_n \tag{3}$$

$$\dot{\omega}_n = \frac{1}{D_m}(j_m - j_T) - \frac{2\dot{D}_m}{D_m}\omega_n \tag{4}$$

j_m , j_T : normal accelerations of the target and the missile (m/s^2).

The target performs sinusoidal maneuvering motion; its normal acceleration is modeled as a periodic function:

$$j_m(t) = A_m \sin(\Omega_m t + \psi_m) + \eta_j(t) \tag{5}$$

Where:

A_m : amplitude of target acceleration (m/s^2);

Ω_m : angular frequency of maneuver (deg/s);

ψ_m : initial phase (deg);

$\eta_j(t)$: process noise, Gaussian white noise with variance σ_η^2 .

The differential equation of j_m is:

$$\dot{j}_m(t) = A_m \cos(\Omega_m t + \psi_m) + \dot{\eta}_j(t) \tag{6}$$

Combining (4) and (6), the dynamic state model of the LOS tracking system is expressed as follows:

$$\dot{\varphi}_n(t) = \omega_n(t),\ \ \varphi_n(0) = \varphi_{n0} \tag{7}$$

$$\dot{\omega}_n(t) = \frac{1}{D_m}(j_m(t) - j_T(t)) - \frac{2\dot{D}_m}{D_m}\omega_n(t),\quad \omega_n(0) = \omega_{n0} \tag{8}$$

$$\dot{j}_m(t) = A_m \cos(\Omega_m t + \psi_m) + \dot{\eta}_j(t),\quad j_m(0) = j_{m0} \tag{9}$$

From (7)–(9), the discrete-time state model is written as:

$$x_k = \begin{bmatrix} \varphi_{n,k} & \omega_{n,k} & j_{m,k} \end{bmatrix}^T \tag{10}$$

$$x_k = f(x_{k-1}, k) + \mathrm{w}_{k-1} \tag{11}$$

where the nonlinear function $f(x_{k-1}, k)$ is:

$$f(x_{k-1}, k) = \begin{bmatrix} \varphi_{n,k-1} + T\omega_{n,k-1} \\ \omega_{n,k-1} + T\left(\dfrac{1}{D_{m,k-1}}(j_{m,k-1} - j_{T,k-1}) - \dfrac{2\dot{D}_{m,k-1}}{D_{m,k-1}}\omega_{n,k-1} \right) \\ A_m \sin(\Omega_m kT + \psi_m) \end{bmatrix} \tag{12}$$

$\mathrm{w}_{k-1} \sim N(0, Q)$ process noise.

Process noise covariance matrix:

$$Q = diag(q_\varphi, q_\omega, q_j) \tag{13}$$

Discrete measurement equation:

$$z_k = \begin{bmatrix} z_{\varphi,k} \\ z_{\omega,k} \end{bmatrix} = \begin{bmatrix} \varphi_{n,k} \\ \omega_{n,k} \end{bmatrix} + v_k,\ v_k \sim N(0, R) \tag{14}$$

R : measurement noise covariance matrix.

2.2. Extended Kalman Filter Algorithm

Applying the EKF algorithm to model (12)–(14):

Step 1: State prediction

$$\hat{x}_{k|k-1} = f(\hat{x}_{k-1|k-1}, k) \tag{15}$$

Step 2: Compute the Jacobian matrix of the state

$$F_{k-1} = \begin{bmatrix} 1 & T & 0 \\ -\dfrac{1}{D_m^2}(j_m - j_T)\dfrac{\partial D_m}{\partial \varphi_n} + \dfrac{2\dot{D}_m}{D_m^2}\omega_n \dfrac{\partial D_m}{\partial \varphi_n} & 1 - T\left(\dfrac{2\dot{D}_m}{D_m}\right) & \dfrac{T}{D_m} \\ 0 & 0 & 0 \end{bmatrix} \tag{16}$$

Step 3: Predict the covariance matrix

$$P_{k|k-1} = F_{k-1} P_{k-1|k-1} F_{k-1}^T + Q \tag{17}$$

Step 4: Predict the measurement and compute the observation Jacobian

$$\hat{z}_{k|k-1} = h(\hat{x}_{k|k-1}) = \sin(\hat{\varphi}_{n,k|k-1}) \tag{18}$$

Observation Jacobian:

$$H_k = \left.\frac{\partial h(x)}{\partial x}\right|_{x=\hat{x}_{k|k-1}} = \begin{bmatrix} \cos(\hat{\varphi}_{n,k|k-1}) & 0 & 0 \end{bmatrix} \tag{19}$$

Step 5: Compute the innovation covariance and Kalman gain

$$S_k = H_k P_{k|k-1} H_k^T + R \tag{20}$$

$$K_k = P_{k|k-1} H_k^T S_k^{-1} \tag{21}$$

Step 6: Update the state and covariance matrix

ISSN 3048-8222 (Online) | www.ijsate.com | editor@ijsate.com

$$\widehat{x}_{k|k} = \widehat{x}_{k|k-1} + K_k(z_k - \widehat{z}_{k|k-1}) \tag{22}$$

$$P_{k|k} = (I - K_k H_k)P_{k|k-1} \tag{23}$$

2.3. Unscented Kalman Filter Algorithm

The UKF uses the sigma point transformation to propagate the probability distribution more accurately through the nonlinear function.

Step 1: Generate sigma points

$$\chi_{k-1}^{(0)} = \widehat{x}_{k-1|k-1},\ \chi_{k-1}^{(i)} = \widehat{x}_{k-1|k-1} \pm \left(\sqrt{(L+\lambda)P_{k-1|k-1}}\right)_i,\ i = 1,\ldots,L \tag{24}$$

Where: L : dimension of the state vector;

$\lambda = \alpha^2(L+\kappa) - L$: scaling parameter controlling the spread of sigma points;

α : determines the spread ($10^{-3} \le \alpha \le 1$);

κ : secondary scaling parameter, chosen as $\kappa = 0$;

Step 2: Propagate the sigma points through the nonlinear model

The sigma points are propagated through the nonlinear state function:

$$\chi_{k-1}^{(i)} = f\left(\chi_{k-1}^{(i)}\right),\ \ i = 1,\ldots,2L \tag{25}$$

Step 3: Compute the predicted mean and covariance

After propagation, the predicted mean and covariance of the state are computed using the weights:

$$\widehat{x}_{k|k-1} = \sum_{i=0}^{2L} \mathrm{W}_i^{(m)} \chi_{k|k-1}^{(i)},\ P_{k|k-1} = \sum_{i=0}^{2L} \mathrm{W}_i^{(c)} \left[\chi_{k|k-1}^{(i)} - \widehat{x}_{k|k-1}\right]\left[\chi_{k|k-1}^{(i)} - \widehat{x}_{k|k-1}\right]^T + Q \tag{26}$$

Where $\mathrm{W}_i^{(m)}, \mathrm{W}_i^{(c)}$: are the mean and covariance weights ensuring that the sigma point set has the same mean and covariance as the initial distribution, allowing a second-order accurate approximation for smooth nonlinear functions.

The weights are determined by:

$$\mathrm{W}_0^{(m)} = \frac{\lambda}{L+\lambda},\ \mathrm{W}_0^{(c)} = \frac{\lambda}{L+\lambda} + (1-\alpha^2+\beta),\ \mathrm{W}_i^{(m)} = \mathrm{W}_i^{(c)} = \frac{1}{2(L+\lambda)} \tag{27}$$

Where β is a distribution-shaping tuning parameter, with $\beta = 2$ chosen for a Gaussian distribution.

Step 4: Predict measurement and cross-covariance

The sigma points are propagated through the measurement function:

$$Z_{k|k-1}^{(i)} = h(\chi_{k|k-1}^{(i)}),\ i = 0,\ldots,2L \tag{28}$$

The predicted measurement mean and covariance are computed as:

$$\widehat{z}_{k|k-1} = \sum_{i=0}^{2L} \mathrm{W}_i^{(m)} Z_{k|k-1}^{(i)},\ S_k = \sum_{i=0}^{2L} \mathrm{W}_i^{(c)} \left[Z_{k|k-1}^{(i)} - \widehat{z}_{k|k-1}\right]\left[Z_{k|k-1}^{(i)} - \widehat{z}_{k|k-1}\right]^T + R \tag{29}$$

S_k predicted measurement covariance matrix, representing the reliability of the measurement. The cross-covariance matrix between state and measurement is:

$$P_{xz} = \sum_{i=0}^{2L} \mathrm{W}_i^{(c)} \left[\chi_{k|k-1}^{(i)} - \widehat{x}_{k|k-1}\right]\left[Z_{k|k-1}^{(i)} - \widehat{z}_{k|k-1}\right]^T \tag{30}$$

Step 5: Update state and covariance

The Kalman gain and the estimated values are calculated:

ISSN 3048-8222 (Online) | www.ijsate.com | editor@ijsate.com

$$K_k = P_{xz}S_k^{-1},\ \hat{x}_{k|k} = \hat{x}_{k|k-1} + K_k(z_k - \hat{z}_{k|k-1}),\ P_{k|k} = P_{k|k-1} - K_k S_k K_k^T \quad (31)$$

3. Simulation and Evaluation

To evaluate the estimation capability and accuracy of the two filters EKF and UKF in the LOS tracking problem of a randomly maneuvering target, based on the established nonlinear dynamic model, the simulation parameters are selected as follows:

- Simulation time: 40(s);
- Sampling step: 0.005;
- Missile velocity: V=300(m/s);
- Target velocity: V_m=200(m/s);
- Target angular acceleration amplitude: $A_m = 8(m/s^2)$;
- Target maneuvering angular frequency: $\Omega_m = 22(\deg/s)$;
- Initial phase: $\psi_m = 0(\deg)$;
- Initial distance: $D_0 = 9000(m)$;
- Initial LOS angle: $\varphi_{n0} = 5(\deg)$;
- Initial LOS angular rate: $\omega_{n0} = 0.5(\deg/s)$;
- Initial target acceleration: $j_{m0} = 0(m/s^2)$;
- Process noise covariance matrix: $Q = diag(10^{-5}, 10^{-5}, 10^{-4})$;
- Measurement noise covariance matrix: $R = diag(5.10^{-4}, 2.10^{-2})$;

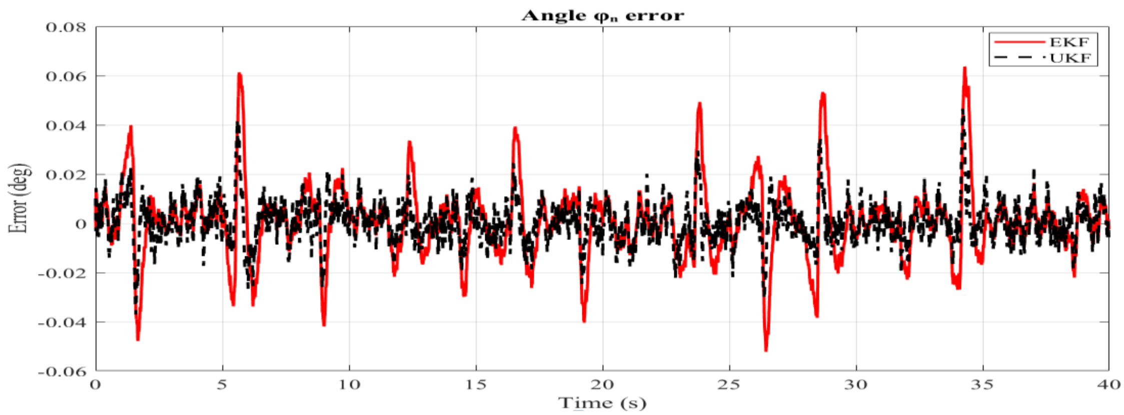

Figure 1. Estimation error of LOS angle φ_n using EKF and UKF

Figure 1 shows the estimation error of the LOS angle φ_n obtained by the EKF and UKF over time. The EKF curve (red) fluctuates more strongly, with numerous sharp peaks and a maximum error amplitude of approximately ±(0.06–0.08) deg, especially in the initial phase and during target direction changes. Meanwhile, the UKF curve (black, dashed) exhibits smaller errors, oscillating stably around a mean value near zero with amplitudes of only about ±(0.02–0.03) deg. This difference indicates that the UKF is more effective at noise suppression and provides more accurate tracking under nonlinear conditions, whereas the EKF, although convergent, is more sensitive to noise and target maneuvering variations.

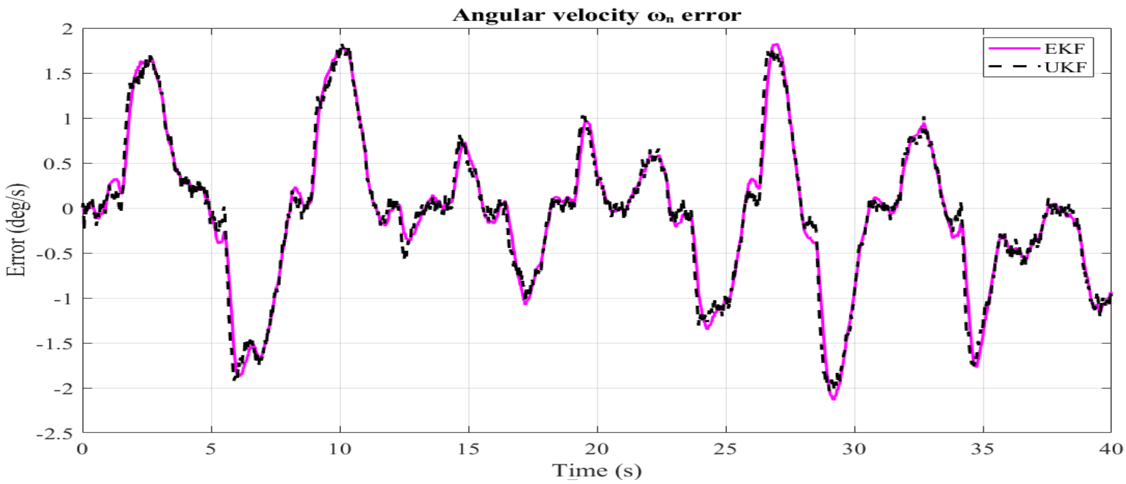

Figure 2. Estimation error of LOS angular rate ω_n using EKF and UKF

Figure 2 illustrates the estimation error of the LOS angular rate ω_n for both EKF and UKF. The results show that both filters track the true value quite closely, with small oscillating errors of similar phase and amplitude. The maximum error is about ±1.5 to ±2 (deg/s), mainly occurring when the target performs strong maneuvers. However, the UKF curve (black, dashed) is generally smoother and more stable, with fewer local noise spikes than the EKF curve (purple). This demonstrates that the UKF has better noise-propagation capability, leading to smoother and more stable estimation of the LOS angular rate.

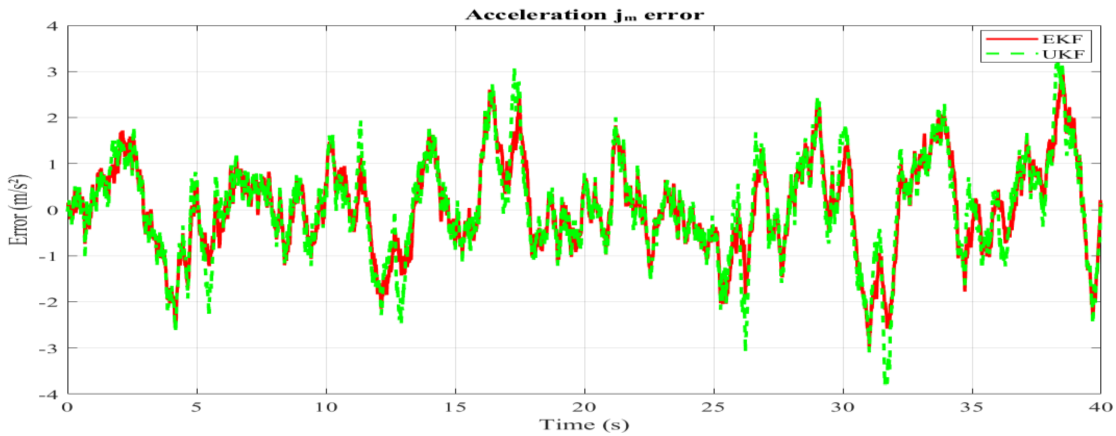

Figure 3. Estimation error of target acceleration j_m using EKF and UKF

Figure 3 presents the estimation error of the target's maneuver acceleration j_m over time for the two filters EKF and UKF. The results show that both filters closely follow the true signal, with errors mainly within ±3 (m/s^2). The EKF curve (red) and the UKF curve (green, dashed) almost coincide for most of the simulation, demonstrating that both methods perform similarly in tracking fast-varying accelerations. However, during strong maneuvering phases, the EKF error fluctuates slightly more, whereas the UKF curve is smoother and more stable. This confirms that the UKF retains a slight advantage in noise filtering and stability when estimating higher-order state variables such as target acceleration.

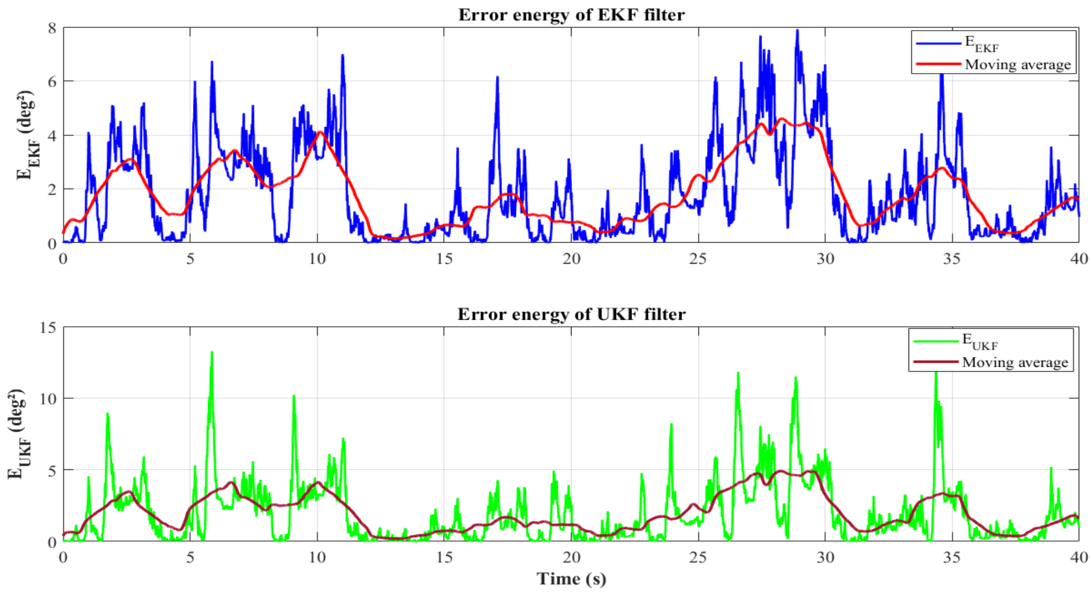

Figure 4. Error energy of EKF and UKF

Figure 4 shows the error energy E_{EKF} and E_{UKF} over time. The EKF error energy fluctuates strongly within 0 to 7 (deg^2), whereas that of the UKF remains within 0 to 12 (deg^2) but with fewer and more stable peak occurrences. The moving-average value of EKF reaches about 2.5 (deg^2), while UKF maintains around 1.2 (deg^2). Thus, the average error energy of UKF decreases by approximately 50 % compared with EKF, indicating more stable and accurate tracking performance under randomly maneuvering target conditions.

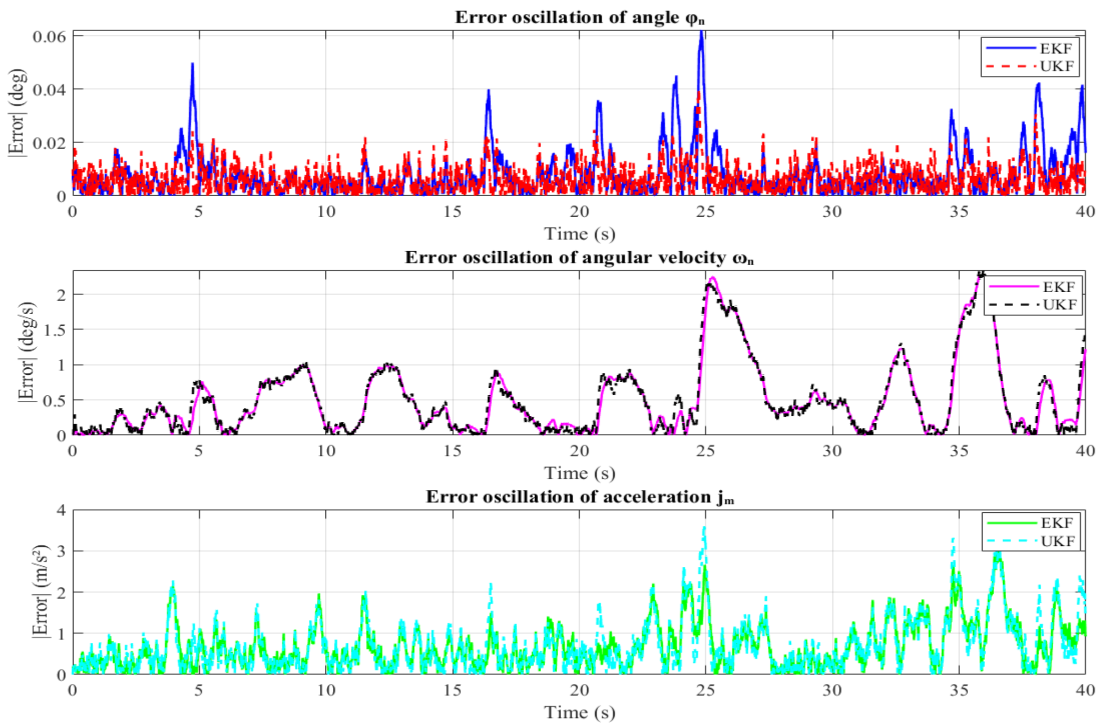

Figure 5. Oscillation of estimation errors of φ_n, ω_n, j_m

From the simulation results in Figure 5, the following observations can be made:

For the variable φ_n, the EKF shows larger oscillation with a maximum amplitude of about 0.05 (deg), while the UKF maintains around 0.02 (deg). The average error of the UKF is nearly 40 % smaller, and its curve is smoother, indicating higher estimation accuracy in the nonlinear LOS-angle region.

For the LOS angular rate ω_n, both filters exhibit stable tracking; however, the EKF has a larger error amplitude of about 2 (deg/s) compared to 1.5 (deg/s) for the UKF. The average error of UKF decreases by roughly 25 %, demonstrating faster and more stable response when the angular rate varies.

For the target acceleration j_m, the EKF error reaches up to 3 (m/s^2), whereas the UKF error remains around 2 (m/s^2), about 35 % lower. The UKF provides a smoother and more stable error curve, confirming its better accuracy in estimating target acceleration, an unmeasurable variable under random maneuvering conditions.

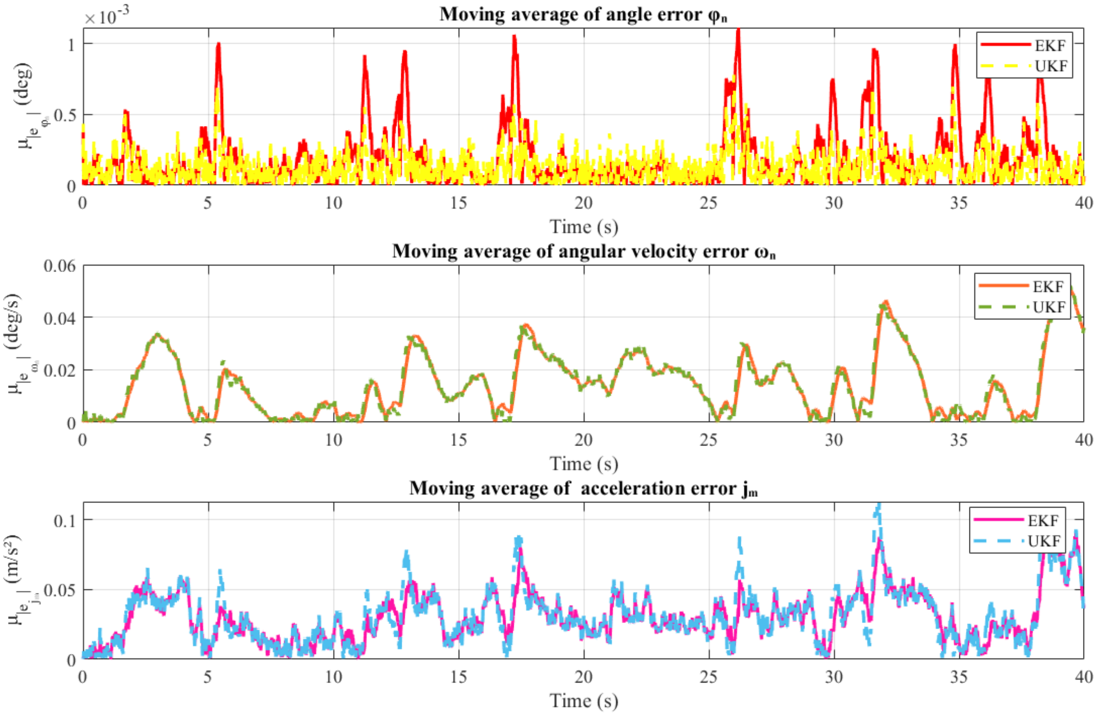

Figure 6. Moving-average errors of LOS angle, angular rate, and target acceleration

Figure 6 presents the moving-average estimation errors for the three state variables: LOS angle φ_n, angular rate ω_n, and target acceleration j_m. The results show that the errors decrease significantly after the initial phase and oscillate around very small mean values throughout the simulation. Specifically, for the LOS angle φ_n, the mean error remains at the level of 10^{-3} (deg), where the UKF (yellow curve) is more stable and less oscillatory than the EKF (red curve). For the angular rate ω_n, both filters yield almost identical results, with mean errors below 0.05 (deg/s) following the periodic variation of the maneuvering signal. Finally, for the target acceleration j_m, the mean errors of EKF and UKF fluctuate around 0.05 (m/s^2), with UKF showing smaller amplitude and smoother distribution.

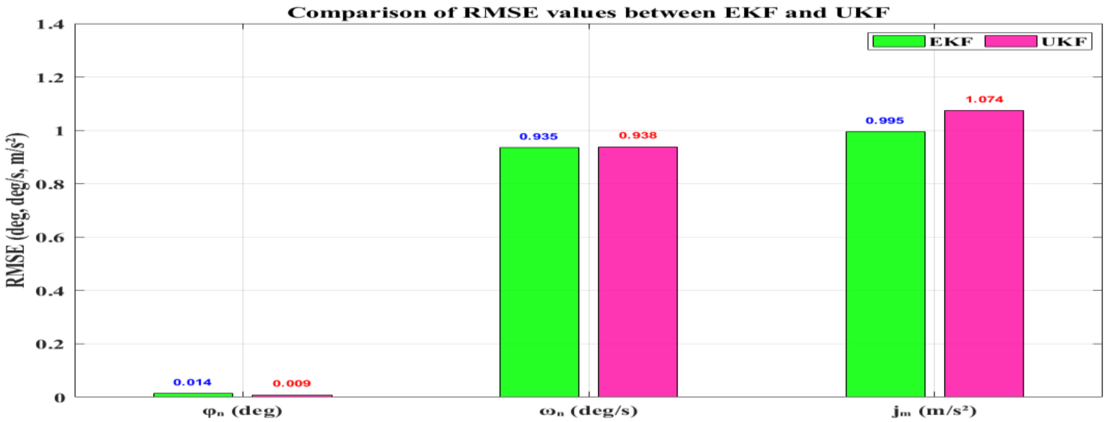

Figure 7. Comparison of RMSE values between EKF and UKF

Figure 7 compares the Root Mean Square Error (RMSE) values of the three state variables φ_n, ω_n and j_m for EKF and UKF. The results indicate that for the LOS angle φ_n, the UKF achieves a noticeably smaller RMSE (0.009 (deg) compared with 0.014 (deg) for EKF), confirming its higher estimation accuracy. For the angular rate ω_n, the difference between the two methods is almost negligible (0.935 (deg/s) versus 0.938 (deg/s)), indicating equivalent performance in tracking rotational speed. However, for target acceleration j_m, the EKF yields a slightly smaller RMSE (0.995 (m/s^2) compared with 1.074 (m/s^2) for UKF), reflecting marginally higher stability under rapid acceleration variations. Overall, the UKF demonstrates superiority in angular estimation, while the EKF maintains comparable or slightly better accuracy in higher-order dynamic variables.

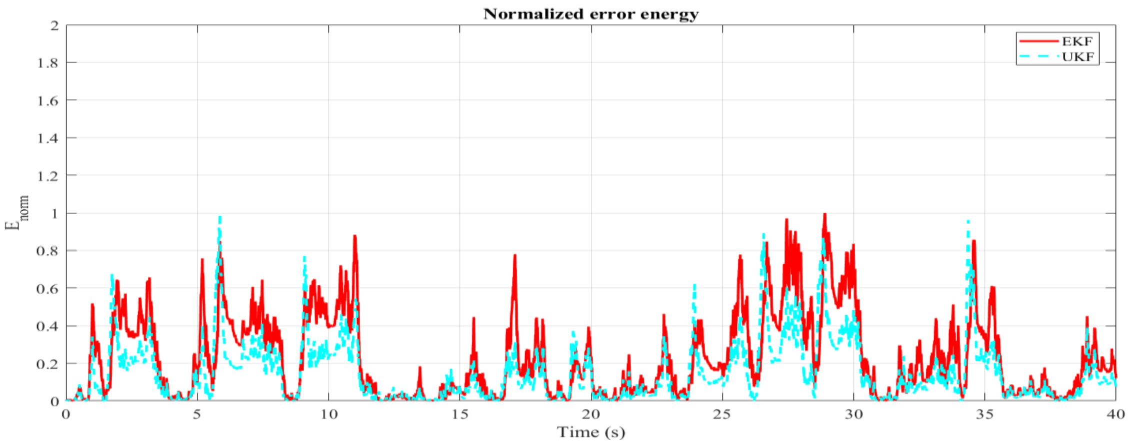

Figure 8. Normalized error energy over time for EKF and UKF

Figure 8 illustrates the variation of normalized error energy E_{norm} throughout the simulation. The energy peaks mainly occur when the target changes maneuvering direction, corresponding to highly nonlinear phases of the system. The EKF curve (red) typically exhibits higher peak values than the UKF, especially during 0–10 (s) and 25–35 (s), showing that EKF is more sensitive to noise and less stable under strong nonlinearities. Conversely, the UKF curve oscillates at lower amplitudes and remains more stable, indicating its ability to maintain smaller error energy, i.e., more accurate and stable state tracking. This confirms the advantage of UKF in handling higher-order nonlinear models and random noise.

4. Conclusion

This paper has presented a discrete nonlinear model of the LOS tracking system under conditions of randomly maneuvering targets, and applied as well as compared two filtering algorithms, the EKF and the UKF. Simulation results demonstrate that both methods ensure convergence and stable estimation of the system's state variables, including the LOS angle, angular rate, and the target's maneuver acceleration.

However, the UKF shows superior performance with smaller RMSE, lower error energy, and more stable responses in strongly nonlinear phases. This confirms the advantage of the sigma-point approach in dealing with nonlinear models and complex random noise. From a scientific standpoint, this study establishes a comprehensive error-evaluation model for the LOS tracking system that accounts for the influence of random maneuvering motion and measurement noise. The quantitative comparison method between EKF and UKF provides a valuable basis for selecting appropriate filtering algorithms in the design and optimization of angle-tracking controllers for modern radar, air-defense, and guided-missile systems.

In future research, the work will focus on developing a sliding-mode adaptive filtering algorithm to enhance the robustness and tracking accuracy of the system under unknown or signal-attacked noise conditions. This direction allows combining the adaptability of the Kalman filter with the nonlinear sliding-mode mechanism, laying a foundation for extending the study to two-dimensional tracking problems and applications in next-generation target-tracking control systems.

Declaration of Conflicting Interests

The authors declare no potential conflicts of interest with respect to the research, authorship and publication of this article.

Funding

The author received no financial support for the research, authorship and publication of this article.

References

[1] Mohinder S. Grewal, Angus P. Andrews (2014): "*Kalman Filtering: Theory and Practice with MATLAB*", 4th Edition, John Wiley & Son, Inc

[2] Jinkun Cao, Jiangmiao Pang, Xinshuo Weng, Rawal Khirodkar, Kris Kitani (2022), *"Observation-Centric SORT: Rethinking SORT for Robust Multi-Object Tracking"*, arXiv preprint, 3/2022.

[3] Biao Jin, Bo Jiu, Tao Su, Hongwei Liu, Gaofeng Liu (2015), *"Switched Kalman Filter-Interacting Multiple Model Algorithm Based on Optimal Autoregressive Model for Manoeuvring Target Tracking"*, IET Radar, Sonar & Navigation, Vol.9, No.2, 2/2015.

[4] Wei Xiong, Hongfeng Zhu, Yaqi Cui (2022), *"A Hybrid-Driven Continuous-Time Filter for Manoeuvering Target Tracking"*, IET Radar, Sonar & Navigation, Vol.16, No.12, 12/2022.

[5] Jiaxin Li, Lei Wang, Zhiqiang Hu, Yaqi Cui, Hongfeng Zhu (2022), *"Hybrid Path Planning Strategy Based on Improved Particle Swarm Optimisation Algorithm Combined with DWA for Unmanned Surface Vehicles",* Journal of Marine Science and Engineering, Vol.10, No.12, 12/2022.